Available at www.sciencedirect.com

ScienceDirect

journal homepage: www.elsevier.com/locate/he

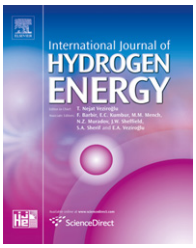

Flameless combustion for hydrogen containing fuels

Yu Yu, Wang Gaofeng, Lin Qizhao, Ma Chengbiao, Xing Xianjun*

Department of Thermal Science and Energy Engineering, University of Science and Technology of China, Hefei 230027, P.R. China

ARTICLE INFO

Article history:
Received 14 April 2009
Accepted 18 April 2009
Available online 29 May 2009

Keywords:
Flameless combustion
Hydrogen containing fuels
NO_x emission
Flue gas recirculation

ABSTRACT

In this paper, flameless combustion was promoted to suppress thermal-NO_x formation in the hydrogen-high-containing fuel combustion. The PSRN model was used to model the flameless combustion in the air for four fuels: H_2/CH_4 60/40% (by volume), H_2/CH_4 40/60%, H_2/CH_4 20/80% and pure hydrogen. The results show that the NO_x emissions below 30 ppmv while CO emissions are under 50 ppmv, which are coincident with the experimental data in the ''clean flameless combustion'' regime for all the four fuels. The simulation also reveals that CO decreases from 48 ppmv to nearly zero when the hydrogen composition varies from 40% to 100%, but the NO_x emission is not sensitive to the hydrogen composition. In the highly diluted case, the NO_x and CO emissions do not depend on the entrainment ratio.

1. Introduction

Dilemma of Energy crisis and pollutant emission causes serious social problems, which challenge the traditional energy utilization patterns. To solve these problems, a high quality energy model named hydrogen energy is proposed to replace the traditional one. By coal or biomass gasification, hydrogen containing fuels (HCFs) can be attained to generate the electricity in the fuel cells or to obtain the thermal energy by direct combustion [1]. Because of the high adiabatic flame temperature of the HCFs, NO_x emission may be largely produced via the thermal-NO_x mechanisms [2]. Recently, a promising low NO_x emissions technique is developed to reduce the flame temperature and the pollutant formations for HCFs, in terms of Flameless Combustion, FLOX, MILD combustion, HiTAC and Diluted combustion [3–7]. Flameless combustion technology characterizes strong internal flue gas recirculation by high-velocity air jet flow entrainment. It could reduce the flame temperature simultaneously reducing NO_x emissions and offering homogeneous temperature field. While decreasing the residence time and the oxygen concentration in the high temperature reaction zone, the temperature gradient and the hot spots in the combustor are suppressed. Thus the thermal-NO_x emissions, which are mainly produced in the temperature above 1500 °C, can be reduced to a low level.

To realize the flameless combustion mode, two prerequisites are suggested by Wunning [3]. First, the fuel and the oxidizer should be preheated to a threshold temperature before the reaction takes place or the furnace temperature should be high enough. Second, sufficient flue gas is entrained into the fresh reactants prior to the combustion. Derudi and Villani [8] reported the T-Kv diagram of the flameless combustion mode for coke oven gas (CH_4/H_2 40/60% by volume) experimentally. They found that the ''clean flameless combustion'', in which NO_x is below 30 ppmv and CO is below 50 ppmv, could be achieved when the fuel and air nozzles were specially designed to obtain the required dilution ratio and jet velocity values. Cavaliere [4] discussed that the flameless combustion was characterized by a volume reaction regime, which indicates the combustion can be modelled by the perfect stirred reactor (PSR). Moreover, Mancini et al. [9]

* *Corresponding author*. Tel.: +86 551 3600430.
E-mail address: qlin@ustc.edu.cn (L. Qizhao).

0360-3199/$ – see front matter © 2009 Professor T. Nejat Veziroglu. Published by Elsevier Ltd. All rights reserved.
doi:10.1016/j.ijhydene.2009.04.036

pointed out that the error predictions of the entrainment were responsible to the underprediction of the entrainment of the burnt gas using a PSR model for methane fuel. They argued that the NO_x production in the near-field of the combustor was mostly caused by the mixing of the burnt gas and incoming fresh reactants. However, few studies have been done on the simulation of flameless combustion for HCFs in the combustor of different flue gas entrainment. Further analysis is needed to classify the key impact to sustain the flameless combustion for the fuels of different hydrogen composition.

In this work, the flameless combustion of H_2/CH_4 80%/20% by vol., H_2/CH_4 60/40% by vol., H_2/CH_4 40%/60% by vol. and pure hydrogen in the combustor of different flue gas recirculation was investigated. Flameless combustion for different HCFs/air was examined to identify the effect of the threshold values of flue gas recirculation and furnace temperature. The effect of Hydrogen composition to the production of NO_x and CO emissions was also discussed.

2. Numerical model

To simulate the flameless combustion process, a series of PSR model was used in which the flue gas entrainment was accounted for as the additional variables inside the reactor [9]. The Chemkin 4.0 code [10] was chosen to calculate the temperature and relatively pollutant formations. Compared to the PSRN model for methane, the network of HCFs–air combustion model consisted of three PSR models. As shown in Fig. 1, burnt gas generated in the latter PSR was partly circulated into the former one. The internal flue gas entrainment ratio was defined as the ratio of the internal mass flow rate of burnt gas to that of the reactants [3]. In these cases, it remained 30% in the fuel side, which was usually used in the calculation of the swirling or high momentum multi-jet combustor. The detailed descriptions of the model were listed in Table 1.

As shown in Fig. 1, the recycling from PSR3 to PSR1 was introduced to represent the dilution of the burnt gas to fresh fuel. The entrainment Kv in the oxidizer side was simulated from an additional inlet. Diluted air was simulated here by the addition of the inert gas to the reactants before the combustion takes place. For the case in this study, the entrainment Kv was calculated by the Equation (1) [8]. Nitrogen instead of the burnt gas was used as the inert gas.

$$Kv = \frac{M_i + M_a + M_f}{M_a + M_f} \tag{1}$$

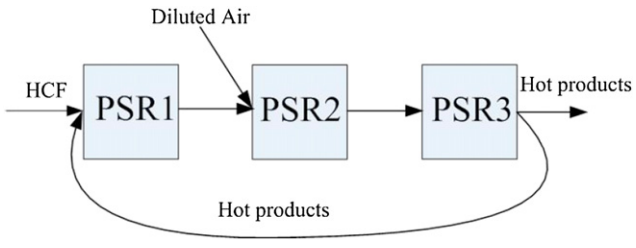

Fig. 1 – The network of perfectly stirred reactors for HCFs.

Table 1 – Detailed parameters of the PSRN model for different HCFs.

Fuel (%)		Flow (g/s)		Excess air ratio
H_2	CH_4	m_{fuel}	m_{air}	
40	60	0.1596	17.1051	1.1
60	40	0.1164	13.3708	1.1
80	20	0.0733	9.6303	1.1
100	0	0.0301	6.8058	1.1

where M_i is the mass flow of the inert gas, M_a is the mass flow of the air and M_f is the mass flow of fuel.

The NO_x was estimated by the well known Zel'dovich mechanism with the following steps [2]:

$$N + NO \rightarrow N_2 + O \tag{2}$$

$$N + O_2 \rightarrow NO + O \tag{3}$$

$$N + OH \rightarrow NO + H \tag{4}$$

3. Results and discussion

3.1. *Flameless combustion for HCFs*

In Fig. 2, A T-Kv diagram for both HCFs and hydrocarbon fuels was displayed. It presented the transition path from conventional flame to the flameless mode. The realization of flameless combustion was summarized as follows [11]:

Zone A. To prevent the reaction from quenching, a preheating section or a heat-up step is first provided in the flameless combustor. The furnace temperature is lifted to the values above the auto-ignition temperature of the fuels (more than 1000 K) by the classical flame. Because of the low jet velocity to maintain the conventional flame front, the jet entrainment is kept to a low Kv level.

Zone B. When the furnace temperature is high enough, Kv is elevated by increasing the jet velocity of the reactants. As a result, the local oxygen concentration in the oxidizer side decreases and the jet momentum in the fuel side increases. These lead the flame to be less visible and the average temperature of the furnace falls.

Zone C. The incoming air entrains much burnt gas before it reacts with the fuel. So that the visible flame disappeared and the reaction region extends to the further downstream zone of the combustor. The high Kv benefits the formation of the high temperature and low oxygen environments. But in the case which Kv is larger than 19 the clean flameless combustion mode can't be sustained, especially for the coke oven gas [8].

Zone D. The furnace temperature is reduced to a critical value by the outer cooling or intense heat transfer in the combustor. Thus the reaction will be extinguished because of the temperature drop in the furnace. For methane fuels, the threshold temperature is often below 1300 K, and for coke oven gas (H_2/CH_4 60/40% by vol.) the limit can be shifted to about 1180 K.

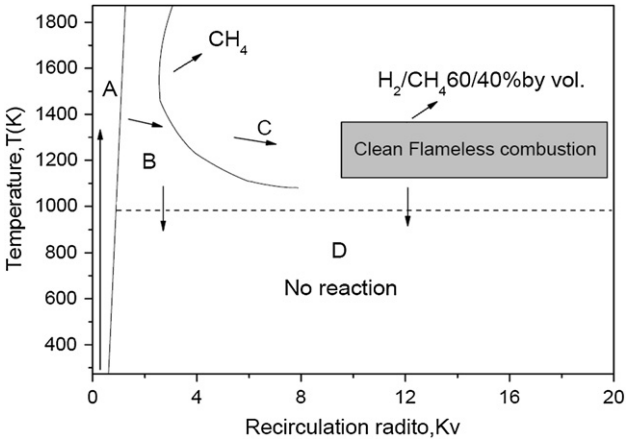

Fig. 2 – Schematic T-Kv diagram for the transition of traditional flame to flameless combustion [2,3]: A, conventional flame; B, transition; C, flameless combustion; D, no reaction.

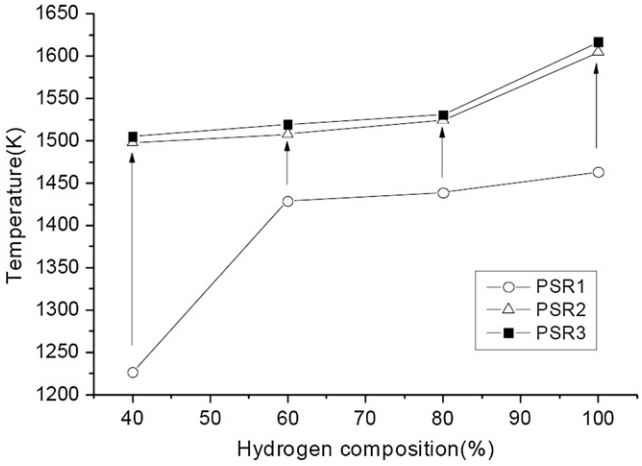

Fig. 3 – Peak temperature, diluted temperature in the fuel and oxidizer sides for different HCFs at Kv = 5.

In order to avoid the formation of the flame front, high jet momentum is adopted to make sure the jet velocity is larger than the flame propagation speed, below which the traditional flame can stabilize in the front of the burner. However, the addition of hydrogen gives a wider flame stability range, and the laminar flame propagation speed increases six times with respect to the methane/air flame [12]. That means higher jet velocity is required when the fuel is supplied from a single nozzle at the constant heat input.

3.2. *Effect of hydrogen composition on the temperature*

In the traditional combustion mode, the addition of hydrogen will increase the adiabatic flame temperature. On the other hand, in the flameless combustion mode the threshold temperature and the proper energy and mass recirculation must be satisfied. As indicated in Fig. 3, the peak temperature, the diluted temperature in the fuel and oxidizer side for different HCFs at Kv = 5 are reported, respectively. In the fuel side, the reactant temperature is elevated to more than 1200 K by 30% of the burnt gas recirculation from the PSR3. And in the oxidizer side, the temperature in the outlet of PSR2 increases about 10 K. It is noteworthy that the high hydrogen composition results in the high temperature increase in the fuel side. But the temperature increased by the reaction between the diluted fuel and air or CH_4/H_2 40%/60% is relatively smaller than the other fuels. This may be determined by the high temperature increase of the entrainment of the burnt gas into the fuels.

3.3. *Effect of hydrogen composition on the CO production and NO_x formation*

The tendency of NO_x and CO emissions varied with the hydrogen composition is shown in Fig. 4. The results show that NO_x emission for all four cases is below 20 ppmv, and CO produced by the reaction of the HCFs and air decreases rapidly by increasing the hydrogen content. It changes from 45 ppmv to nearly zero when the hydrogen composition varies from 40% to 100%. These results also demonstrated that CO emission responses sensitively to the hydrogen amount in the HCFs, corresponding to the experimental data in "clean flameless combustion" mode reported by Derudi and Villani [8].

Note that the NO_x emission simulated in all the case is similar. It suggests in the flameless mode the NO_x emission is less dependent to the hydrogen content of HCFs. As shown in Fig. 3, the NO_x production in PSR2 is slightly higher than that after PSR3. It also illustrates that most of NO_x emission is generated in the reaction of the diluted fuel and air. Because of the decrease of NO_x product, a reburning process may occur in the diluted process of the burnt gas and the fresh fuel.

3.4. *Effect of the entrainment ratio on the temperature and pollution formation*

To explain the formation of the flameless combustion, the temperature and related pollutants are shown in Fig. 5. This figure shows the temperature distribution as well as the NO_x

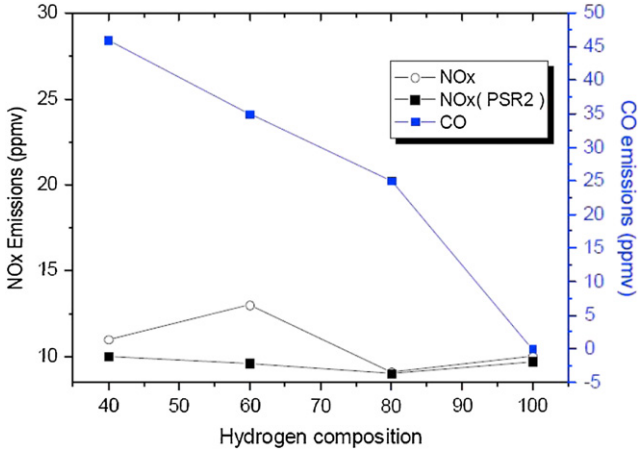

Fig. 4 – Variation of the NO_x and CO emissions for different HCFs at Kv = 5.

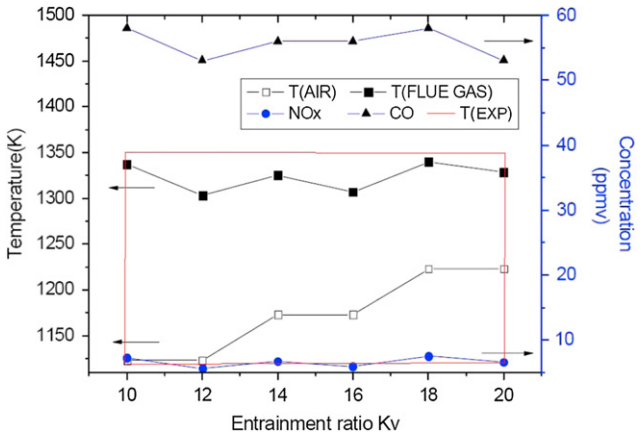

Fig. 5 – NO_x, CO production and temperature profile at different entrainment ratio for CH_4/H_2 60%/40%.

and CO emissions when the entrainment ratio increases. Although the temperature of diluted air increases from 1123 K to 1223 K when the entrainment ratio varies from 10 to 20, the temperature calculated by PSR3 almost remains constant. That means the high entrainment of the inert gas can eliminate the effect of minor increase of diluted air. The CO and NO_x concentrations do not differ greatly from the level in the ''clean flameless combustion'' mode. Little change is observed in the CO and NO_x emissions when the entrainment ratio increases. It suggests that the pollutant does not depend on the entrainment ratio in the high diluted case. Compared to the experimental results reported in the references [13,14], the temperature simulated agrees well with those obtained from the experiment, which is in the threshold of 1123–1353 K. And the CO and NO_x emissions correspond to ''the clean flameless combustion'' regime mentioned above.

4. Conclusion

Flameless combustion for hydrogen containing fuels is investigated by the simulation of the reaction between the diluted fuel and air. The main results are as follows:

Different hydrogen containing fuels can work in the ''clean flameless combustion'' mode, proven by the experimental data and numerical simulation of PSRN model. Above the required threshold temperature and entrainment ratio, flameless combustion can be sustained.

For the fuels with more hydrogen contents, higher peak temperature can be obtained in the flameless combustion process. In the case, both the NO_x and CO emissions calculated by the PSRN model are similar to the experimental data, corresponding to the clean flameless combustion mode.

The pollutant formations are extremely low in the flameless combustion condition for all the fuels studied. In the flameless combustion mode, the CO emission decreases by increasing the hydrogen contents in HCFs, but the NO_x emissions are not sensitive to the hydrogen composition of the HCFs when the furnace temperature and dilution are kept constant. Further analysis reveals that in the highly diluted case, the NO_x and CO emissions do not depend on the entrainment ratio.

REFERENCES

[1] Moriarty P, Honnery D. Intermittent renewable energy: the only future source of hydrogen. Int J Hydrogen Energy 2007; 32:1616–24.
[2] Skottene M, Rian KE. A study of NO_x formation in hydrogen flames. Int J Hydrogen Energy 2007;32:3572–85.
[3] Wunning JG. Flameless oxidation to reduce thermal NO-Formation. Prog Energ Combust 1997;23:81–94.
[4] Cavaliere A. Mild combustion. Prog Energ Combust 2004;30: 329–66.
[5] Milani A, Saponaro A. Diluted combustion technologies. IFRF Combustion Journal 2001;1:1–32.
[6] Rafidi N, Blasiak W. Heat transfer characteristics of HiTAC heating furnace using regenerative burners. Appl Therm Eng 2006;26:2027–34.
[7] Xing X, Wang B, Lin Q. Structure of reaction zone of normal temperature air flameless combustion in a 2.ton/h coal-fired boiler furnace. Proceedings of the I Mech E Part A Journal of Power and Energy 2007;221:473–80.
[8] Derudi M, Villani A. Sustainability of mild combustion of hydrogen-containing hybrid fuels. Proc Combust Inst 2007; 31:3393–400.
[9] Mancinia M, Schwöppea P, Webera R, Orsinob S. On mathematical modelling of flameless combustion. Combust Flame 2007;150:54–9.
[10] Kee RJ, Rupley FM, Miller JA, Coltrin ME, Grcar JF, Meeks E. Theory manual, CHEMKIN release 4.0.1. Reaction Design, Inc.; 2004.
[11] Alessandro C, Galbiati MA, Effuggi A, Gelosa D, Rota R. Mild combustion in a laboratory-scale apparatus. Combust Sci and Tech 2003;175:1347–67.
[12] Di Sarli V, Di Benedetto A. Laminar burning velocity of hydrogen–methane/air premixed flames. Int J Hydrogen Energy 2007;32:637–46.
[13] Yang WH, Blasiak W. Flame entrainments induced by a turbulent reacting jet using high-temperature and oxygen-deficient oxidizers. Energy Fuels 2005;19:1473–83.
[14] Park J, Choi J, Kim S, Kim K, Keel S, Noh D. Numerical study on steam-added mild combustion. Int J Energy Research 2004;28:1197–212.